PHYSICAL REVIEW B **75**, 241302(R) (2007)

Ab initio study of oxygen interstitial diffusion near $Si:HfO_2$ interfaces

Chunguang Tang and Ramamurthy Ramprasad*
Department of Chemical, Materials and Biomolecular Engineering, Institute of Materials Science, University of Connecticut, 97 North Eagleville Road, Storrs, Connecticut 06269, USA
(Received 23 March 2007; published 4 June 2007)

The tendency of oxygen interstitials to diffuse and segregate to the $Si:HfO_2$ interface is evaluated by performing first principles interstitial formation and migration energy calculations at various distances from the interface. A coherent $Si:HfO_2$ heterostructure based on monoclinic HfO_2 was used in this study. These computations indicate that strong thermodynamic and kinetic driving forces exist for the segregation of oxygen interstitials to the interface, providing for a mechanism for the subsequent formation of SiO_x interfacial phases.

DOI: 10.1103/PhysRevB.75.241302 PACS number(s): 68.35.Fx, 68.35.Dv

Due to the current miniaturization trend in microelectronics, high dielectric constant (or high-κ) materials such as HfO_2 and ZrO_2 have gained considerable attention as prospective substitutes for conventional SiO_2 gate dielectrics. One of the critical factors that have led to these choices is the expected thermodynamic stability of HfO_2 and ZrO_2 when in contact with Si. For instance, the following reactions (with M=Hf or Zr) are known to be endothermic:[1–3]

$$MO_2 + Si = M + SiO_2, \quad (1)$$

$$MO_2 + 2Si = MSi + SiO_2. \quad (2)$$

The unfavorable nature of the above reactions is desirable as the formation of silica at $Si:MO_2$ interfaces will decrease the total capacitance and the formation of the silicide will make the $Si:MO_2$ interface metallic.[2]

However, contradictory to the above predictions, the formation of silica, Hf (or Zr) silicide and silicate at the interfaces have been observed.[4–9] Cho *et al.*[4] have found that the formation of Hf silicide is intimately related to the deficiency of oxygen, and Qiu *et al.*[8] have reported transformation of Hf silicide into Hf silicate during a postannealing in oxygen ambient. It has been proposed that these interfacial reactions could be closely related to the presence and high diffusivity of O-based point defects in the metal oxides.[10] In particular Stemmer[10] has shown that the free energy change for Eq. (2) could be negative for ZrO_2 at high temperatures in the presence of oxygen vacancies.

Compared with thermodynamic analysis, which strictly applies only to large systems,[3] first principles modeling enables atomic scale investigation of interfacial structures. In a recent *ab initio* molecular dynamics study of the layer-by-layer growth of HfO_x on Si, Hakala *et al.*[11] have found that O atoms can diffuse across the interface and form a Si suboxide. Our work constitutes the initial steps towards a closer look at the atomic level driving forces for the formation of such interfacial phases. In a previous study[12] we calculated the formation energies and migration barriers of oxygen vacancies in $Si:HfO_2$ heterostructures and found that there exist strong thermodynamic and kinetic driving forces for the formation of Hf silicides at the interface in the presence of oxygen vacancies. In this work, we have performed a detailed atomic level density functional theory (DFT) based study of the tendency of diffusion of O interstitials in a $Si:HfO_2$ heterostructure. Our results show quantitatively that the segregation of O interstitials to the interface is favored both thermodynamically and kinetically, indicating a preference for the formation of a SiO_x ($0<x<2$) layer at the interface in the presence of O interstitials.

In the present work, we consider epitaxial, coherent $Si:HfO_2$ heterostructures with HfO_2 in the monoclinic phase. Although experimentally grown HfO_2 on Si is amorphous, and not epitaxial, we believe that the general conclusions we draw concerning defect chemistries is strongly dependent on the local environment and is less dependent on the specific choice of the HfO_2 phase. In fact, our previous study of O vacancies in $Si:HfO_2$ heterostructures with HfO_2 in tetragonal, pseudotetragonal and monoclinic phases have yielded similar results.[12] This previous study has also shown that monoclinic HfO_2-based epitaxial $Si:HfO_2$ heterostructures are the most stable, and are the systems considered here.

DFT calculations were performed using the VASP code[13] with the Vanderbilt ultrasoft pseudopotentials,[14] the generalized gradient approximation (GGA) utilizing the PW91 functional,[15] and a cutoff energy of 400 eV for the plane wave expansion of the wave functions. A Monkhorst-Pack k-point mesh of $4\times4\times1$ was used for the interface models that contained 2 Si atoms per layer, and the k-point mesh was proportionately decreased for larger supercells.

Our epitaxial $Si:HfO_2$ heterostructures [Fig. 1(a)] were constructed by placing a (001) monoclinic HfO_2 slab on a (001) Si slab such that the [100] direction of HfO_2 coincide with that of Si. The lattice constants a and b of HfO_2 were stretched to match the equilibrium GGA Si lattice constant of 5.46 Å. The top (Hf) and bottom (Si) free surfaces of the heterostructures were passivated with half monolayer of O atoms, thereby passivating all dangling bonds at the surfaces.[16] O-terminated interfaces were considered here, as these have been shown earlier to be the most stable ones.[16] The models contained 9 Si, up to 8 Hf and 18 O layers, and about 10 Å of vacuum separated the heterostructure slabs from their periodic images along the slab surface normal. After geometry optimization, half of the interface O atoms contributed to the formation of Si-O-Si bonds, while the other half resulted in Hf-O-Hf bonds, as shown in Fig. 1(a). This configuration allows for the passivation of all interface atoms as prescribed by the bond counting arguments of Peacock and Robertson.[16] HfO_2 far from the interface contained

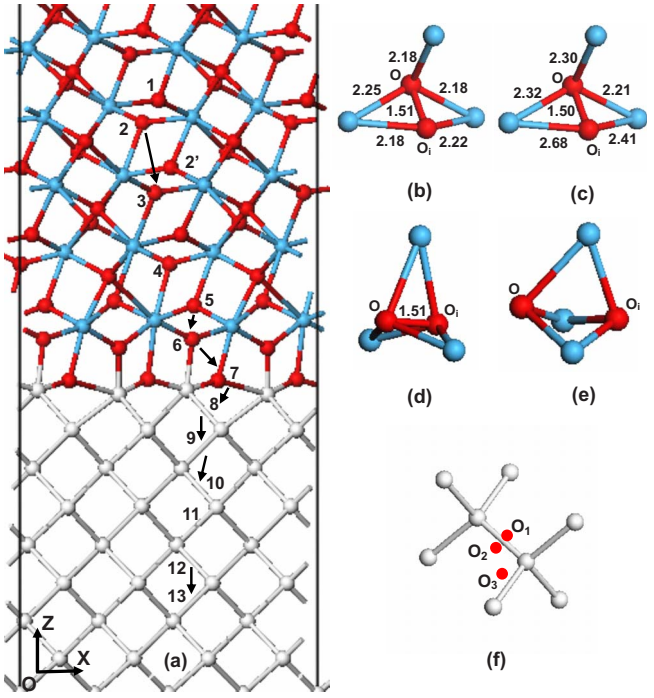

FIG. 1. (Color online) (a) $Si:HfO_2$ heterostructure with Si, Hf, and O atoms shown in white, blue (gray), and red (dark gray), respectively. Isolated O interstitials were created near labeled sites, and arrows represent the migration pathways for O interstitials. (b) and (c) show the oxygen interstitial (O_i) configuration in unstrained and strained bulk HfO_2, respectively. (d) and (e) show the high- and low-energy O interstitial configurations associated with site 5. (f) Possible locations of interstitial atomic O (red dot) in Si lattice.

both threefold and fourfold coordinated O atoms while near the interface all O atoms were threefold coordinated.

O interstitial formation energies were then calculated for four parts of the heterostructure: (1) the HfO_2 part far from the $Si:HfO_2$ interface, with labels 1–3 in Fig. 1(a), (2) the part close to the interface, but on the HfO_2 side, with labels 5–7, (3) the part close to the interface, but on the Si side, with labels 8–11, and (4) the Si part far from the interface, with labels 12, 13. Cases (1) and (4) were treated using bulk HfO_2 and Si supercells, as the atomic structure about 5 Å away from the interfaces on either direction were identical to the corresponding bulk. In all cases, the O interstitial formation energy E_{form} was defined as $E_{\text{form}}=E_{\text{int}}-E_{O_2}/2-E_{\text{perf}}$, where E_{int}, E_{O_2}, and E_{perf} are the energy of the system with an O interstitial, the energy of an isolated O_2 molecule, and the energy of an interstitial-free perfect system, respectively.

O interstitial calculations in bulk HfO_2 were computed using a 97 atom supercell. The equilibrium lattice constants of bulk monoclinic HfO_2 were determined to be 5.14, 5.19, and 5.30 Å, in good agreement with experiments.[17] Here, we consider the "strained" monoclinic structure whose a and b lattice constants were constrained at the Si lattice constant of 5.46 A (corresponding to an optimized c lattice constant of 5.11 A). O interstitials in equilibrium monoclinic bulk HfO_2 could be bound to a threefold or a fourfold coordinated lattice O atom. Foster *et al.*[18] have determined E_{form} for these two cases to be 1.6 and 2.3 eV, respectively. Our results for these two cases are 1.75 and 2.48 eV, respectively, for the equilibrium bulk, and 0.95 and 0.66 eV, respectively, for the strained bulk. In view of the small difference in E_{form} for the strained bulk and that all O atoms near the $Si:HfO_2$ interface are threefold coordinated, we consider only the threefold coordinated case here. In both the strained and unstrained bulk HfO_2, the threefold coordinated lattice O, which initially is in the plane defined by its three neighboring Hf atoms, moves away from the plane and the interstitial O in order to accommodate the latter. The lattice O, the interstitial O and their three neighboring Hf atoms form two tetrahedra that share the triangle base formed by Hf atoms, as shown in Figs. 1(b) and 1(c). In both the strained and unstrained cases the distances between the lattice and the interstitial O atoms are about 1.50 Å. As shown in the figures, the distances between O and Hf atoms in the strained case are larger than those in the unstrained case, which provides more space to accommodate the interstitial O and thus decreases the E_{form} in the strained bulk HfO_2.

To compute the E_{form} of O interstitials near the interface, we consider a $Si:HfO_2$ heterostructure supercell with a 10.92×10.92 Å^2 area along the interface plane and inserted an O interstitial near a threefold coordinated O labeled as 5, 6, and 7 in Fig. 1(a), corresponding to the third, second, and interfacial O layers, respectively. The HfO_2 near the interface featured two possible lattice-interstitial oxygen pair configurations. In the first type of configuration [Fig. 1(d)], the O-O bond length was about 1.50 Å, similar to the bulk HfO_2 case, while in the second type [Fig. 1(e)], the O-O distance was more than 2.3 Å. For the first type of configuration, the E_{form} values associated with sites 5, 6, and 7 were computed to be 0.93, 1.41, and 0.75 eV, respectively, while for the second type, the corresponding values are −0.75, −1.01, and −0.47 eV, respectively. It appears that near the interface the separation of the lattice O and the interstitial O atoms is preferable over the formation of oxygen pair. This result is different from the case for the $Si:SiO_2$ interface where the lattice O atom (initially bridging two Si atoms) and the interstitial O atom prefer to form a peroxy linkage rather than two separate Si-O-Si bonds.[19] It is interesting to note that the bond length of the peroxy O-O bond in SiO_2 is 1.51 Å,[20] same as that of the lattice-interstitial oxygen pair in HfO_2.

O interstitials on the Si side were created by inserting an O atom at bridging positions labeled as 8, 9, 10, and 11, respectively, between two neighboring Si atoms, as shown in Fig. 1(a). After relaxation the Si-O-Si bonds possess a puckered shape. Corresponding to each site label, we considered two possible bridging positions with different distance of the O atom from the interface [e.g., sites O_1 and O_2 in Fig. 1(f), see migration discussion below]. While in bulk Si, the O_1 and O_2 interstitial positions are equivalent by symmetry, this is not the case close to the interface. The E_{form} values for sites 8–11 for O interstitial in the O_1/O_2 position were computed to be −2.90/−2.78, −2.46/−2.57, −2.92/−3.02, and −2.81/−2.83 eV, respectively.

Finally we computed E_{form} in bulk Si to be −2.66 eV using a supercell of 64 Si atoms, which is in fair agreement with previous calculations.[21,22]

The fact that E_{form} decreases from positive values in bulk HfO_2 to negative values in HfO_2 near the interface to large

TABLE I. Interstitial formation (E_{form}) and migration (E_{migr}) energies (eV) in Si:HfO_2 heterostructure. Refer to Fig. 1 for the labels of interstitial sites and migration paths. The two values for E_{form} near the interface refer to the two O-O binding modes on the HfO_2 side of the interface, and the two symmetry inequivalent O interstitial locations on the Si side.

	O_i site	E_{form}	Migr. path	E_{migr}
unstrained			1 to 2	0.79
bulk	1, 2 and 3	1.75	2 to 3	1.43
HfO_2				
strained			1 to 2	0.48
bulk	1, 2 and 3	0.95	2 to 3	0.50
HfO_2			2 to 2′	1.88
	5	0.93/−0.75	5 to 6	0.45
	6	1.41/−1.01	6 to 7	0.55
near	7	0.75/−0.47	7 to 8	0
interface	8	−2.90/−2.78	8 to 9	2.34
	9	−2.46/−2.57	9 to 10	2.44
	10	−2.92/−3.02		
	11	−2.81/−2.83		
bulk Si	12 and 13	−2.66	12 to 13	2.26

negative values in the Si side of the interface reflects the thermodynamic driving force for the tendency of O interstitials to migrate from the bulk HfO_2 to bulk Si. Whether this will happen in reality will be determined by barriers to the migration of O interstitials from site to site, i.e., the kinetic factors.

In order to address the kinetic aspects in detail, we performed O interstitial migration calculations using the nudged elastic band method.[23] For all migration calculations we employed the same supercells as those for E_{form} calculations. Energy barriers for migration, E_{migr}, along the pathways shown by arrows in Fig. 1(a) were determined and their values are shown in Table I.

Foster *et al.*[24] have studied the migration mechanisms of O interstitials in bulk HfO_2 and have identified two possible mechanisms: the exchange and the interstitial mechanisms. In the exchange mechanism the diffusing O interstitial replaces a lattice O which then becomes the new diffusing O interstitial. The interstitial mechanism involves the diffusion of an O interstitial through the space between the lattice sites. Foster *et al.* found that the migration barrier for the exchange mechanism (0.8 eV) was 0.5 eV lower than that for the interstitial mechanism. We reproduced the exchange diffusion process within a 97-atom HfO_2 supercell, in which the O interstitial bound to the lattice O at site 2 (Fig. 1) displaces the lattice O at site 1 by moving along a direction roughly parallel to the (001) (or interface) plane. The barrier for this $2 \rightarrow 1$ exchange migration process computed here for the unstrained and strained bulk HfO_2 cases were 0.78 and 0.48 eV, respectively. We also considered the migration of O interstitial from near site 2 to near site 3 via the interstitial mechanism. This process involved a barrier of 0.50 eV (compared with 1.43 eV for the unstrained supercell). Thus, in the strained bulk HfO_2, the barriers for the exchange and interstitial mechanisms are nearly equal. However, we only consider the interstitial mechanism in the present work for the following two reasons: (1) the diffusion path of the exchange mechanism ($2 \rightarrow 1$) is roughly parallel to the interface plane, while that of the interstitial mechanism ($2 \rightarrow 3$) is roughly normal to the interface plane and (2) owing to the larger diffusion distance along $2 \rightarrow 3$ compared to $2 \rightarrow 1$, the barrier for exchange diffusion along the former path which is directed toward the interface is expected to be higher. Site 2′ is yet another neighbor to site 2. However, the barrier for an O interstitial to migrate from site 2 to 2′ was 1.88 eV (in the strained bulk), significantly higher than that of site 2 to site 3 migration. The latter direction, in addition to having a low migration energy, can recursively cause the motion of an O interstitial from the bulk HfO_2 part to the interface.

Migration energies were computed for O interstitials on the HfO_2 side of the Si:HfO_2 interface, for migration from site 5 to site 6, and from site 6 to site 7. These were 0.45 eV and 0.55 eV, respectively, when the beginning and end point geometries corresponded to the low energy configurations discussed earlier (i.e., with long O-O distances).

The diffusion of an O interstitial from site 7 to site 8 involved crossing the Si:HfO_2 interface, and was found to occur spontaneously, i.e., with no barrier. Subsequent migration of the O interstitial into successive Si layers involved large barriers (2.34 and 2.44 eV). It was mentioned earlier that associated with a given labeled O site on the Si side of the Si:HfO_2 interface are two positions [locations marked as O_1 and O_2 in Fig. 1(f)] which are inequivalent close to the interface but equivalent by symmetry in bulk Si. Migration of the O interstitial between these positions was not considered although barriers for migration from one of them to the nearest bridge site below [e.g., from O_2 to O_3 in Fig. 1(f)] was computed. The barrier for O interstitial diffusion in bulk Si was computed to be 2.26 eV, which is in excellent agreement with prior calculations.[25] The small barriers (of less than 0.5 eV) for O interstitial diffusion on the HfO_2 side of the Si:HfO_2 interface, the barrierless migration across the interface, and the large barriers (greater than 2.2 eV) on the Si side of the interface indicates that O interstitials will segregate to the interface and remain at the first layer of Si below HfO_2. This may, in part, explain the oxidation of interfacial Si-Si bond observed in a recent *ab initio* molecular dynamics simulation of the layer-by-layer growth of HfO_x on Si.[11]

All the barrier values along with the interstitial formation energies, listed in Table I, were used to create an O interstitial migration energy profile shown in Fig. 2. All energies in this figure represented as square symbols correspond to those of the "images" of the nudged elastic band computations (i.e., initial, final, and intermediate geometric configurations during migration). Energies are defined relative to (E_{perf} $+E_{O_2}/2$), so that the energies of the initial/final images (labeled by numbers) correspond to interstitial formation energies. The energy profile pictorially captures *both* the thermodynamic and kinetic driving forces for the segregation of O interstitials to the Si side of the Si:HfO_2 interface.

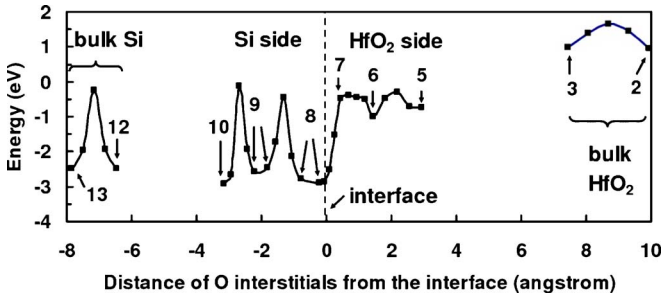

FIG. 2. (Color online) O interstitial migration profiles for $Si:HfO_2$ heterostructure.

In summary, we have performed detailed first principles computations to capture the atomic level diffusion tendencies of O interstitials in $Si:HfO_2$ heterostructures. Our conclusion is that strong thermodynamic *and* kinetic driving forces exist for O interstitials to segregate to and get trapped at the interfacial Si layers. An important implication of these calculations is that the presence of O interstitials in HfO_2 could lead to the formation of a thin interfacial SiO_x layer between Si and HfO_2.

The authors would like to acknowledge financial support of this work by the ACS Petroleum Research Fund.

*Email address: rampi@uconn.edu

[1] R. M. Wallace and G. D. Wilk, CRC Crit. Rev. Solid State Mater. Sci. **28**, 231 (2003).
[2] J. Robertson, Rep. Prog. Phys. **69**, 327 (2006).
[3] J.-P. Locquet, C. Marchiori, M. Sousa, J. Fompeyrine, and J. W. Seo, J. Appl. Phys. **100**, 051610 (2006).
[4] D. Y. Cho, K. S. Park, B. H. Choi, S. J. Oh, Y. J. Chang, D. H. Kim, T. W. Noh, R. Jung, J. C. Lee, and S. D. Bu, Appl. Phys. Lett. **86**, 041913 (2005).
[5] H. S. Baik, M. Kim, G.-S. Park, S. A. Song, M. Varela, A. Franceschetti, S. T. Pantelides, and S. J. Pennycook, Appl. Phys. Lett. **85**, 672 (2004).
[6] R. Jiang, E. Q. Xie, and Z. F. Wang, Appl. Phys. Lett. **89**, 142907 (2006).
[7] J.-C. Lee, S.-J. Oh, M. Cho, C. S. Hwang, and R. Jung, Appl. Phys. Lett. **84**, 1305 (2004).
[8] X. Y. Qiu, H. W. Liu, F. Fang, M. J. Ha, and J. M. Liu, Appl. Phys. Lett. **88**, 072906 (2006).
[9] N. Miyata, Appl. Phys. Lett. **89**, 102903 (2006).
[10] S. Stemmer, J. Vac. Sci. Technol. B **22**, 791 (2004).
[11] M. H. Hakala, A. S. Foster, J. L. Gavartin, P. Havu, M. J. Puska, and R. M. Nieminen, J. Appl. Phys. **100**, 043708 (2006).
[12] C. Tang, B. Tuttle, and R. Ramprasad (unpublished).
[13] G. Kresse and J. Furthmuller, Phys. Rev. B **54**, 11169 (1996).
[14] D. Vanderbilt, Phys. Rev. B **41**, R7892 (1990).
[15] J. P. Perdew, J. A. Chevary, S. H. Vosko, K. A. Jackson, M. R. Pederson, D. J. Singh, and C. Fiolhais, Phys. Rev. B **46**, 6671 (1992).
[16] P. W. Peacock, K. Xiong, K. Tse, and J. Robertson, Phys. Rev. B **73**, 075328 (2006).
[17] J. Adam and M. D. Rodgers, Acta Crystallogr. **12**, 951 (1959).
[18] A. S. Foster, F. Lopez Gejo, A. L. Shluger, and R. M. Nieminen, Phys. Rev. B **65**, 174117 (2002).
[19] T. Akiyama and H. Kageshima, Appl. Surf. Sci. **216**, 270 (2003).
[20] A. Bongiorno and A. Pasquarello, Phys. Rev. B **70**, 195312 (2004).
[21] J. L. Gavartin, L. Fonseca, G. Bersuker, and A. L. Shluger, Microelectron. Eng. **80**, 412 (2005).
[22] J. Coutinho, R. Jones, P. R. Briddon, and S. Öberg, Phys. Rev. B **62**, 10824 (2000).
[23] G. Henkelman and H. Jonsson, J. Chem. Phys. **113**, 9978 (2000).
[24] A. S. Foster, A. L. Shluger, and R. M. Nieminen, Phys. Rev. Lett. **89**, 225901 (2002).
[25] M. Ramamoorthy and S. T. Pantelides, Phys. Rev. Lett. **76**, 267 (1996).